Design framework for high-speed 3D scanning tools and development of an axial focusing micromirror-based array

Ersumo, Nathan Tessema, Yalcin, Cem, Antipa, Nick, Pégard, Nicolas, Waller, Laura, et al.

Nathan Tessema Ersumo, Cem Yalcin, Nick Antipa, Nicolas Pégard, Laura Waller, Daniel Lopez, Rikky Muller, "Design framework for high-speed 3D scanning tools and development of an axial focusing micromirror-based array," Proc. SPIE 11293, MOEMS and Miniaturized Systems XIX, 1129303 (28 February 2020); doi: 10.1117/12.2550994

SPIE.

Event: SPIE OPTO, 2020, San Francisco, California, United States

Design Framework for High-Speed 3D Scanning Tools and Development of an Axial Focusing Micromirror-Based Array

Nathan Tessema Ersumo*[a,b], Cem Yalcin[b], Nick Antipa[b], Nicolas Pégard[c], Laura Waller[b,d], Daniel Lopez[e], and Rikky Muller[a,b,d]

[a]University of California, Berkeley - University of California, San Francisco Graduate Program in Bioengineering, USA, [b]Departement of Electrical Engineering & Computer Sciences, University of California, Berkeley, CA, USA 94720, [c]Department of Applied Physical Sciences, University of North Carolina at Chapel Hill, Chapel Hill, NC, USA 27514, [d]Chan Zuckerberg Biohub, San Francisco, CA, USA 94158, [e]Center for Nanoscale Materials, Argonne National Laboratory, Lemont, IL, USA 60439

ABSTRACT

Rapid 3D optical scanning of points or patterned light is widely employed across applications in microscopy, material processing, adaptive optics and surveying. Despite this broadness in applicability, embodiments of 3D scanning tools may vary considerably as a result of the specific performance needs of each application. We present here a micromirror array-based modular framework for the systemic design of such high-speed scanning tools. Our framework combines a semi-custom commercial fabrication process with a comprehensive simulation pipeline in order to optimally reconfigure pixel wiring schemes across specific applications for the efficient allocation of available degrees of freedom. As a demonstration of this framework and to address existing bottlenecks in axial focusing, we produced a 32-ring concentric micromirror array capable of performing random-access focusing for wavelengths of up to 1040 nm at a response rate of 8.75 kHz. By partitioning the rings into electrostatically driven piston-mode pixels, we are able to operate the array through simple open-loop 30 V drive, minimizing insertion complexity, and to ensure stable operation by preventing torsional failure and curling from stress. Furthermore, by taking advantage of phase-wrapping and the 32 degrees of freedom afforded by the number of independently addressable rings, we achieve good axial resolvability across the tool's operating range with an axial full-width-half-maximum to range ratio of 3.5% as well as the ability to address focus depth-dependent aberrations resulting from the optical system or sample under study.

Keywords: MEMS, micromirrors, 3D scanning, high-speed, systematic design

1. INTRODUCTION

1.1 3D optical scanning

The dynamic 3D translation of patterned light, such as an individual focused light spot or an entire point cloud volume, has applications across a number of disciplines (Figure 1). In neurobiology, such laser scanning techniques can be employed to target actuating and sensing probes for volumetric single-cell resolution recording and/or stimulation.[1] In the realm of fabrication, laser micromachining[2] and maskless lithography[3] can also be achieved with optical patterning at microscopic scales via 3D scanning. And at macro-level spatial scales, 3D scanning is critical to optical surveying methods including LiDAR.[4] Lastly, from an adaptive optics perspective, fields including astronomy[5] and ophthalmoscopy[6] rely on 3D scanning because dynamic focusing corrects for defocus aberrations while dynamic beamsteering allows for fine resolution wavefront correction by sweeping across sub-fields of view. Across all of these applications, there is a distinct benefit to scanning at high speeds as it translates to higher throughput for optical targeting and actuation, for the acquisition of sensing and recording data, and for the processing of materials into desired products.[2,7]

Despite the ubiquity of optical scanning across disciplines, specific embodiments of 3D scanning tools vary widely and in accordance with the diversity in performance needs across applications. Two important specifications driving this variety are the lateral (XY) and axial (Z) dimensions of both the whole volume and elemental pattern of interest. Taken together, these specifications set the number of spatially distinct locations that the unit pattern can be targeted to across the full volume of interest. In addition, while in principle only 3 modes of control are required for 3D scanning (Figure 1), additional degrees of freedom may be required for a given application to address target position-dependent aberrations

MOEMS and Miniaturized Systems XIX, edited by Wibool Piyawattanametha, Yong-Hwa Park, Hans Zappe, Proc. of SPIE Vol. 11293, 1129303 · © 2020 SPIE · CCC code: 0277-786X/20/$21 · doi: 10.1117/12.2550994

stemming from the scanning tool itself, from another component of the optical system being employed, or from the sample/region of interest. For instance, additional radial phase control beyond defocusing may be needed to address target depth-dependent spherical aberrations,[8] and off-axis conditions introduced by beam-steering across large lateral fields may require addressing coma and field curvature aberrations.[9]

Altogether, the simultaneously prevalent and application-specific nature of optical 3D scanning tools warrants an efficient and systematic method of designing such tools using the same versatile platform. First, such a platform should reliably produce high-speed tools that allow for nimble and consolidated operation with low insertion loss. Second, such a development platform should provide the widest possible range for usability, meaning that produced devices should be polarization-independent, operable across a wide range of optical wavelengths, and capable of sustained dwelling. Lastly, this platform must be capable of easily and efficiently apportioning available degrees of freedom in a manner that is highly tailored to specific performance needs. In light of these needs, we present here a MEMS micromirror-based modular framework for the systemic design of scanning tools that combines a comprehensive simulation pipeline with a semi-custom commercial foundry process. We also demonstrate the utility of our framework by using it to develop a micromirror-array based axial focusing tool.

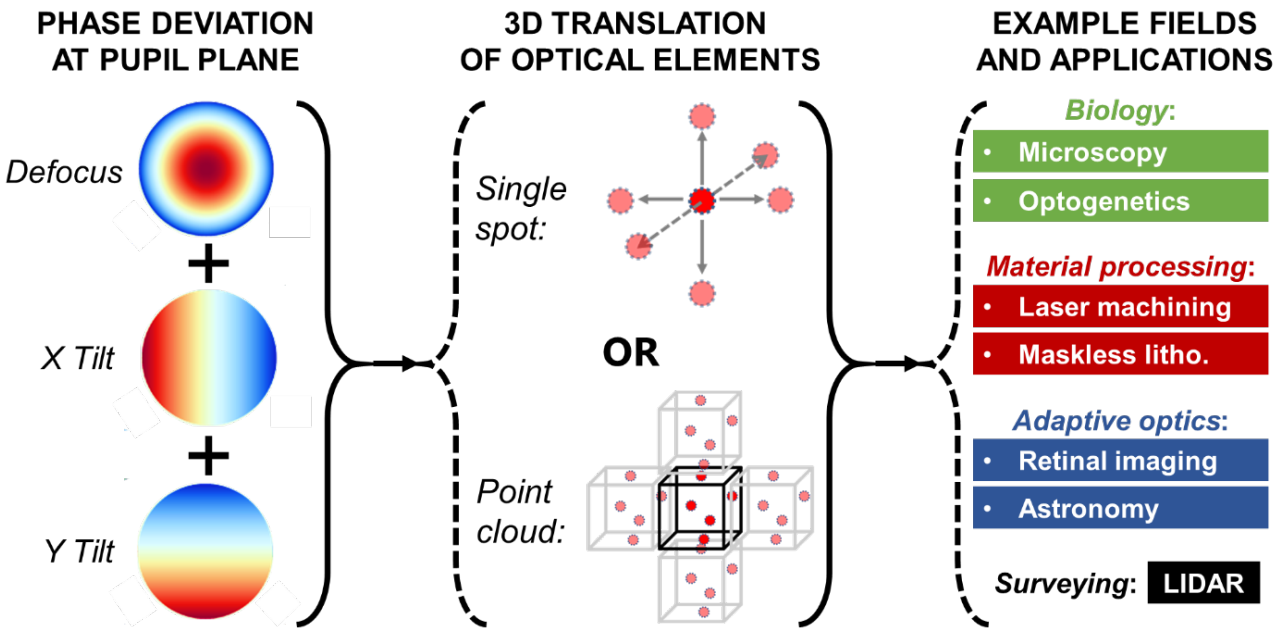

Figure 1. Scanning light spots or entire point clouds across 3D can be performed through pure-phase optical modulation across three parameters, namely the magnitudes of defocusing, x-axis tilting and y-axis tilting, though additional degrees of freedom may be required for additional corrections. Achieving rapid 3D scanning can improve throughput across a number of applications that employ optics for targeting, sensing, correction, or fabrication.

1.2 The axial focusing subtask: a salient bottleneck

While state-of-the-art lateral scanning tools including galvanometer mirrors and acousto-optic deflectors boast refresh rates in excess of 5 kHz (under dwelling-capable non-resonant mode operation),[10] some of the most widely used and commercially available axial focusing tools today are not able to match these speeds. Indeed, dynamic optofluidic lenses[11] and liquid crystal-based devices[12] operate at refresh rates that are well under 300 Hz. Accordingly, efforts have been made to increase axial focusing speeds to refresh rates of up to 1 MHz by employing alternative technologies as shown in Table 1. But these improvements have come at the expense of crucial performance capabilities. Specifically, piezoelectrically or electrostatically driven deformable mirror arrays[13] and electro-optic deflectors[10] require very high voltage drives that entail cumbersome amplifiers, precluding the possibility of compact driver integration. Alternatively, strategies such as cascading acousto-optic deflectors[10,14] or creating zone plates with digital micromirror device (DMD) arrays[15] drastically

reduce transmission efficiency. Furthermore, tunable acoustic gradient index of refraction (TAG) lenses[16] are continuously sweeping across z, which means that laser syncing is required and dwelling is not possible. In addition, monolithic MEMS mirror plates require resonant-mode operation for meaningful operating ranges, which severely limits performance under dwelling-capable non-resonant modes.[17] And lastly, most of these approaches to axial focusing offer no additional degree of freedom, constraining their ability to address target position-dependent aberrations and thereby limiting the ease with which they can be fully adapted to various systems. Therefore, overall, our survey of existing scanning technologies identifies axial focusing as the most salient bottleneck today, lagging behind lateral scanning tools in high-speed scanning applications, which is why we chose it as the target application for a prototype demonstration of our framework.

Table 1. Comparison of high-speed axial focusing technologies. DMD: digital micromirror device. TAG: tunable acoustic gradient index of refraction. RF AM: radio frequency amplitude modulation.

	Deformable mirror arrays[13]	**Tunable electro-optic lenses**[10]	**Zone plate focusing with DMDs**[15]	**Cascaded acousto-optic deflectors**[10,14]	**TAG lenses**[16]	**Monolithic MEMS mirror plates**[17]
Refresh rate	1-50 kHz	1 MHz	50 kHz	1 MHz	1 MHz	>100 kHz
Driving range	>250 V	±150 V	2 V	5 V (RF AM)	50 V	20 V
Transmission efficiency	>90%	60-80%	<10%	10-50%	>90%	>90%
Polarization dependence	No	Yes	No	No	No	No
Dwelling capacity	Yes	Yes	Yes	Yes	No	Limited
Degrees of freedom per target depth	Multiple	1	1	1	1	1

2. SYSTEMATIC DESIGN APPROACH

As evidenced by the popularity of galvanometers for lateral scanning and the axial focusing technologies listed in Table 1, the prevailing approach to increasing 3D scanning speeds involves employing mechanical methods to actuate mirrors. Settling times for such systems are determined by mechanical resonant frequency, which scales with $\sqrt{k/m}$ (where k and m are respectively the spring constant and dynamic mass of the actuation mode of interest). By exploiting the surge in resonant frequency that comes from shrinking down to MEMS scales, micromirror structures can achieve refresh rates of 10 kHz or higher.[18] Broadly, mirror-based scanning tools can be classified into monolithic structures (ex: galvanometers and varifocal plates) and multi-actuator arrays. Larger monolithic structures benefit from the simplest driving schemes but, as previously mentioned, provide limited additional control and often rely on resonant-mode operation due to the high drive required of DC operation. On the other hand, micromirror arrays are currently offered at pixel counts on the order of 10^2-10^3 and with continuous membrane structures for mirror support that allow for stable and uniform operation. But the high voltage drives required of such actuators constitute an opportunity cost to driving requirements in applications where stability and spatial uniformity constraints can be relaxed by the averaging benefits of grouped actuator operation. So while high-speed tools of both types are commercially available for off-the-shelf use, the application-specific nature of scanning tasks often results in inefficiencies for such fixed-format tools, with either (a) insufficient levels of control and precision being allocated the most critical degrees of freedom, or (b) excess degrees of freedom that go wasted and created undesired operating overhead.

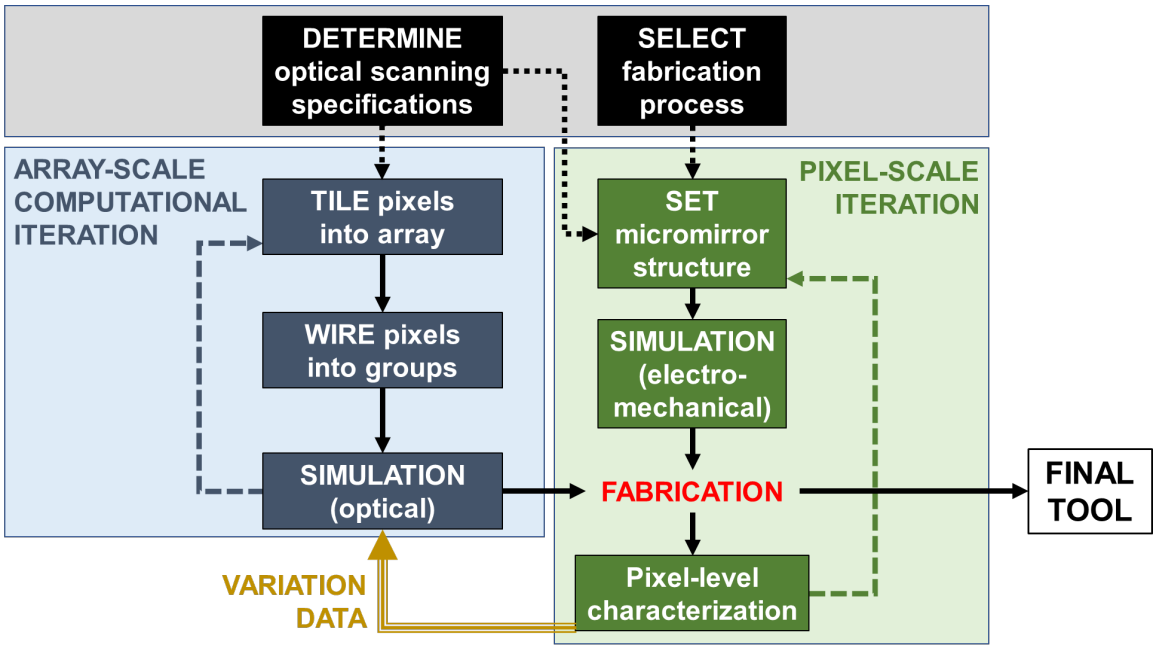

Figure 2. Flowgraph illustrating micromirror-based design approach to optical scanning tools. Once the target tool specifications and fabrication platform are set, pixel-scale and array-scale design iterations can be decoupled for a modular development process.

Accordingly, we propose an object-oriented array-format design approach to mirror-based scanning tools that decouples the building blocks (i.e. micromirror pixels) determining transduction characteristics (ex: applied drive vs. achieved phase shift, settling behavior, etc.), from the array-scale geometry determining overall optical functionality (as shown in Figure 2). This modular design scheme is achieved by fixing the pixel tiling pattern as shown in Figure 3(a) and adjusting grouped wiring schemes between pixels as shown in Figure 3(c). Once the pattern and pitch of the array tiling scheme is set, pixels may be selectively added or removed in accordance with this scheme across a 2D working area that is agnostic to the unit pixel's mechanical structure. First, such a decoupled analysis strategy between unit actuator structure and array configuration provides freedom in setting the transduction mechanism and its balance between spatial uniformity and sensitivity without affecting the array-level phase coordination strategy that determines optical performance. For our prototype axial focusing tool, we designed a piston-mode micromirror pixel[19,20] suspended by two clamped-guided beams (as shown in Figure 3(b)) to achieve a level of sensitivity that allows for full 2π phase shifting across wavelengths of up to 1040 nm with a refresh rate of 8.75 kHz and simple open-loop 30 V drive.[21] However, depending on the application, the unit actuator pixel may be easily switched out within the modular design framework to entirely different structures that rely on alternative mechanisms such as amplitude modulation[22] or diffraction.[23] Second, compared to larger monolithic structures, partitioning active areas of mirror-based scanning tools into co-wired grouped regions and again into small pixels provides improved sensitivity for lower driving ranges, the ability to phase-wrap applied patterns for extended operating ranges, and mitigation against the effects of both residual stress mismatch and instability from unconstrained resonant modes. Third, while segmented micromirror arrays are susceptible to diffraction effects that can introduce unwanted static and dynamic diffraction orders as well as reduce zeroth-order efficiency commensurately with the square of array fill factor,[24] such segmented arrays can be operated in optical setups that eliminate these undesired effects via static illumination patterning and spatial filtering as shown in Figure 3(d).

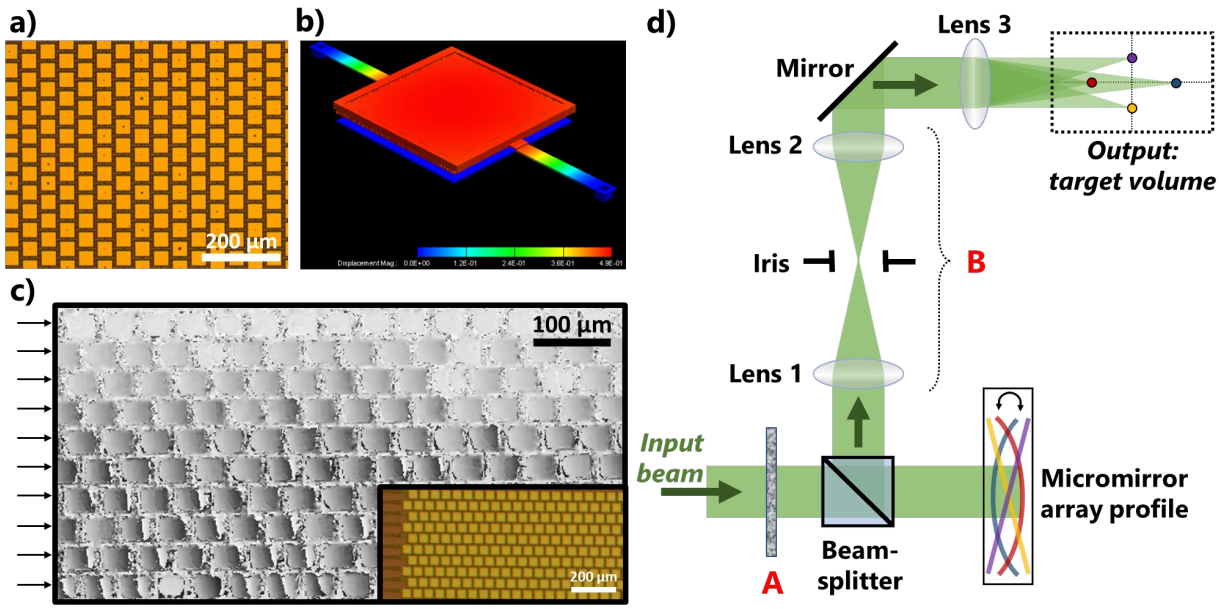

Figure 3. a) Micrograph of fabricated micromirror array showing staggered orthogonal tiling scheme. b) Finite element simulation result (CoventorWare) showing structure and actuation behavior of a unit micromirror pixel. c) Phase reconstruction of sample micromirror array wired into independent rows (as shown with black arrows) and actuated to produce a phase ramp for beamsteering. Microscopy image of array with routing trace to each row shown in bottom-right inset. d) Envisioned optical system for 3D scanning using micromirror arrays. A binary amplitude mask (**A**) may be used to illuminate only active areas of the employed array and a spatial filter (**B**) can be employed to prevent unwanted diffraction orders from appearing around the volume of interest.

3. DESIGN APPROACH IMPLEMENTATION

3.1 Simulation pipeline

Our fabricated array with a staggered orthogonal tiling format (Figure 3(a)) has a diameter of 8.2 mm with a 48 µm pixel pitch, is partitioned into 32 rings, has a 7.2° radial slice removed for the routing of wire traces, and was developed using a simulation pipeline that is at the core of our design framework as shown in Figure 4. Array parameters including pixel fill factor and the reflectivity of both active and static areas of the working region may be adjusted within the pipeline to match chosen fabrication and pixel structure specifications. Subsequently, optical parameters are set by defining the size, shape and wavelength of the incident illumination beam as well as the focal length and placement of the offset lens employed for a default focus position centered at (x,y,z)=(0,0,0). One of the most prominent and useful features of this pipeline is its ability to incorporate intra-pixel and inter-pixel spatial variations in performance based on *a priori* experimentally-obtained distribution data of static topography and dynamic actuation behavior for the chosen pixel structures. Lastly, once this feature has been used to repeatedly generate phase profiles representative of ones produced by actual fabricated arrays (similarly to Monte Carlo algorithms), computational simulations of optical propagation through the system are performed to obtain mean optical performance and expected deviation ranges.

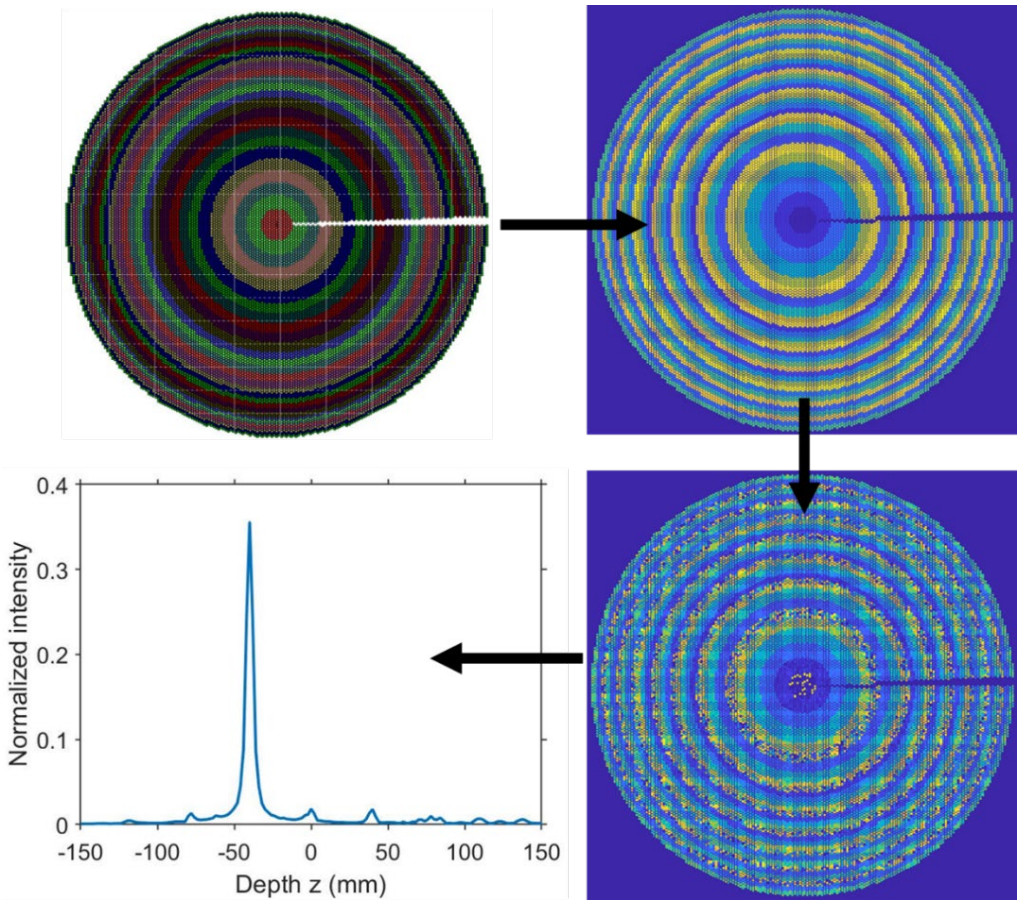

Figure 4. Simulation pipeline for axial focusing array. Using a layout of the fabricated array (*top left*, independent rings shown in different colors), ideal phase masks are first generated for each target focus depth (*top right*). Variations to these ideal phase masks can subsequently be repeatedly introduced to computationally reproduce non-idealities in optical performance due to mismatches in pixel behavior and topography (*bottom right*). Lastly, mean optical performance (on-axis intensity across the z-axis) can be obtained from propagation simulations (*bottom left*). In the context of recording and manipulating cells in biological tissue, such an axial focusing tool would for example require a cell-resolution spot size of ~10 μm or less, a focusing range of up to ~500 μm (as limited by tissue absorption and scattering), and operability across visible light and near-infrared wavelength ranges for single and multi-photon excitation respectively.

3.2 Simulation results

Simulation results for the fabricated axial focusing array are shown in Figure 5. Operating range across the z-axis is defined as the range across which the on-axis peak intensity of the scanned spot is greater than that of other peaks resulting from higher-order diffraction effects. The full width at half maximum ($FWHM_{x,y,z}$) of the scanned spot was used as a measure of spot size. Spot intensity drops as target depth increases in either direction because escalating defocus requires sharper radial phase gradients and, in discrete array systems such as ones with micromirrors, efficiency scales inversely with phase gradient under a $sinc^2$ relationship.[25] We find that the dynamic dioptric power range of the array alone (excluding the contribution of the offset lens) is ±2.89 diopters, which is comparable the ranges of commercially available optofluidic lenses that also make use of offset lenses.[26] In addition, as shown in Figure 5(b), lateral spot dimensions do not deviate significantly from the diffraction-limited spot size set by the aperture, focal length and wavelength of the optical system. Moreover, the discontinuity seen around x=0 in Figure 5(b) is due to the transition from a shallow convex mirror profile with minor pixel actuation around the central array region to a shallow concave mirror profile with extensive actuation around the same central array region. Since variation in pixel behavior increases with the extent of actuation, concave mirror profiles exhibit a slight decrease in focusing performance compared to convex profiles. We note that while the results in Figure 5 were obtained for a specific focal length *f* of the offset lens (200 mm), the $FWHM_z$-to-operating range

ratio can be used as a magnification-independent metric of focusing performance because both axial spot size and operating range scale with f^2. Similar ratios may be also used for the analysis of lateral scanning arrays since lateral spot size and beamsteering range scale with f.

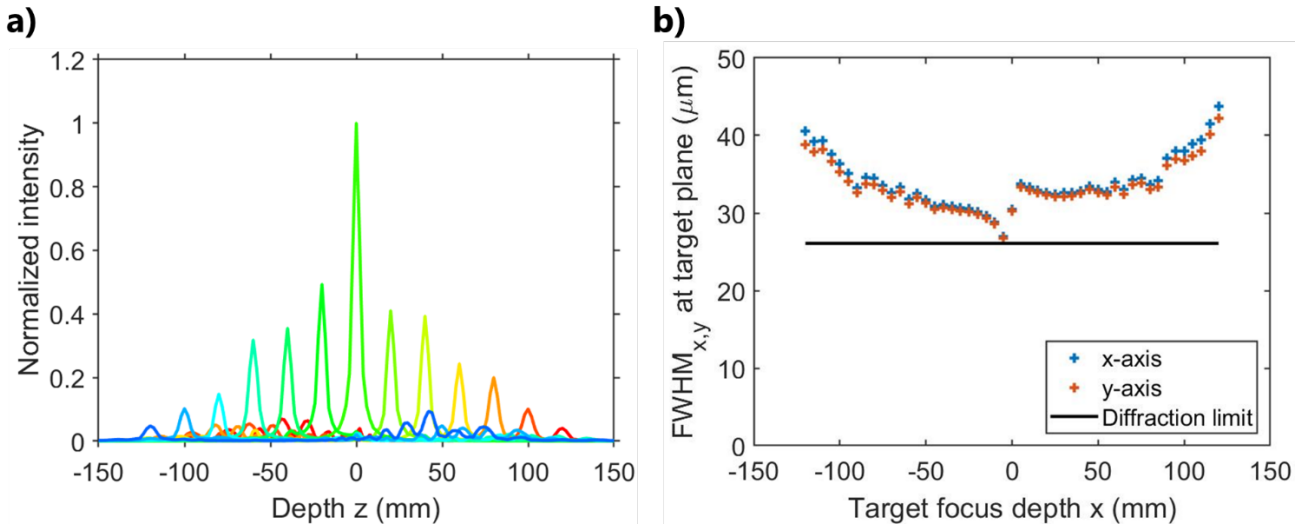

Figure 5. Full simulation results for fabricated axial focusing array using a 1040 nm Gaussian beam for illumination and a 200 mm focal length offset lens. a) On-axis normalized intensity profile for array phase masks across the entire operating range. b) Lateral dimensions (FWHM along x and y axes) of focused spots at their target depths across the operating range. Black line corresponds to the size of a diffraction-limited spot at z=0 for the given array aperture and lens focal length.

4. EXPERIMENTAL PERFORMANCE RESULTS

The designed array was fabricated using MEMSCAP's PolyMUMPs and MUMPs-Plus services, which provides a semi-custom foundry production path that complements our tailorable design framework by offering the option of minor modifications to the general fabrication process flow. Specifically, one thickness modification was made to decrease the driving voltage range by reducing the spring constant of the suspension beams while maintaining robustness against curling from residual stress mismatches in our chosen pixel structures. We subsequently performed chip-level custom post-processing to deposit a 250 nm thick reflective gold layer via evaporation and liftoff.[21] Following board assembly for driver integration and pixel-level characterizations of actuation behavior, we tested axial focusing using a 100 mm offset lens and a camera mounted on an automated axial stage for z-stack acquisitions. Experimental focusing performance results for a number of phase profiles are shown in Figure 6.

5. CONCLUSIONS

We have explored the concept of a micromirror-based, easily reconfigurable design framework for the application-specific efficient allotment of degrees of control in high-speed 3D optical scanning tools. We have also demonstrated a successful design iteration using this framework by producing a concentric micro-mirror array with comparable focusing performance to existing commercial tools but at a higher refresh rate of 8.75 kHz, at a reasonable driving range of 30 V, and without sacrificing key performance capabilities such dwelling capacity, depth-dependent aberration correction, and polarization independence. Given the modularity of this design process, we can feasibly envision building out or modifying this tool with additional features, including: supplementary astigmatism correction or beam-steering capabilities through additional partitioning, limited dynamic runtime rewiring capabilities with electromechanical relays for multi-mode tool operation, and changing the reflective coating to a metasurface for even more compact and synergistic optical performance.

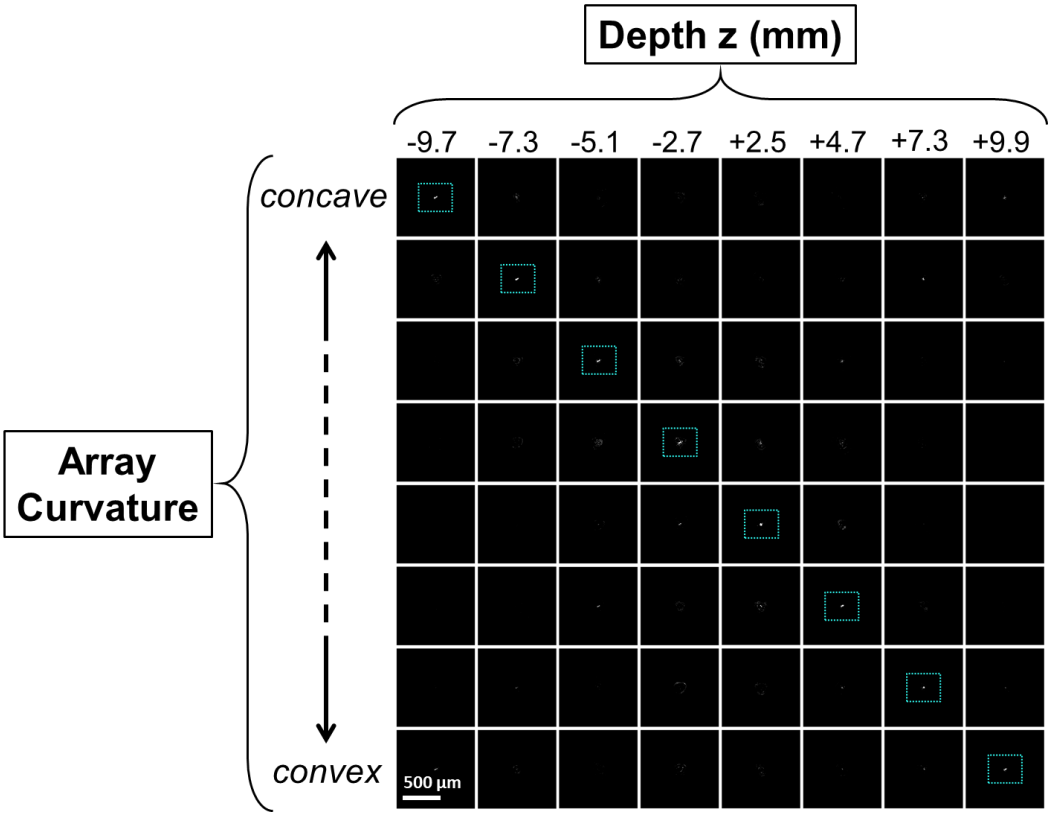

Figure 6. Experimental results demonstrating axial focusing with fabricated concentric array for a 532 nm wavelength collimated source and a 100 mm focal length offset lens. Array rings were actuated to produce different concave and convex phase-wrapped mirror profiles. XY-plane images were acquired for each applied phase profile at multiple depths. Refocused light spots are demarcated here with dashed boxes.

6. ACKNOWLEDGMENTS

The authors thank Prof. Ming Wu, the Marvell Nanofabrication Laboratory and sponsors of the Berkeley Wireless Research Center for tools, equipment and guidance. This work was performed, in part, at the Center for Nanoscale Materials, a U.S. department of Energy Office of Science User Facility, and supported by the U.S. Department of Energy, Office of Science, under Contract No. DE-AC02-06CH11357.

REFERENCES

[1] Emiliani, V., Cohen, A. E., Deisseroth, K. and Häusser, M., "All-Optical Interrogation of Neural Circuits.," J. Neurosci. **35**(41), 13917–13926 (2015).

[2] Chen, T.-H., Fardel, R. and Arnold, C. B., "Ultrafast z-scanning for high-efficiency laser micro-machining," Light Sci. Appl. **7**(4), 17181 (2018).

[3] Wen, S.-B., Bhaskar, A. and Zhang, H., "Scanning digital lithography providing high speed large area patterning with diffraction limited sub-micron resolution," J. Micromechanics Microengineering **28**(7), 75011 (2018).

[4] Hasselbach, J., Bogatscher, S. and Rembe, C., "Laser scanning module with large sending aperture and inherent high angular position accuracy for 3D LiDAR," Opt. Sensors 2019 **11028**, 1102804, International Society for Optics and Photonics (2019).

[5] Matthews, S. A., Collados, M., Mathioudakis, M. and Erdelyi, R., "The European solar telescope (EST)," Ground-based Airborne Instrum. Astron. VI **9908**, 990809, International Society for Optics and Photonics (2016).

[6] Zhang, Y., Poonja, S. and Roorda, A., "MEMS-based adaptive optics scanning laser ophthalmoscopy," Opt. Lett. **31**(9), 1268–1270 (2006).
[7] Yu, Y., Zhang, T., Meadway, A., Wang, X. and Zhang, Y., "High-speed adaptive optics for imaging of the living human eye," Opt. Express **23**(18), 23035 (2015).
[8] Ue, Y., Monai, H., Higuchi, K., Nishiwaki, D., Tajima, T., Okazaki, K., Hama, H., Hirase, H. and Miyawaki, A., "A spherical aberration-free microscopy system for live brain imaging," Biochem. Biophys. Res. Commun. **500**(2), 236–241 (2018).
[9] Potsaid, B., Finger, F. P. and Wen, J. T., "Automation of challenging spatial-temporal biomedical observations with the adaptive scanning optical microscope (ASOM)," IEEE Trans. Autom. Sci. Eng. **6**(3), 525–535 (2009).
[10] Heberle, J., Bechtold, P., Strauß, J. and Schmidt, M., "Electro-optic and acousto-optic laser beam scanners," Laser-based Micro- Nanoprocessing X **9736**, U. Klotzbach, K. Washio, and C. B. Arnold, Eds., 97360L, International Society for Optics and Photonics (2016).
[11] Mishra, K., van den Ende, D., Mugele, F., Mishra, K., Van den Ende, D. and Mugele, F., "Recent Developments in Optofluidic Lens Technology," Micromachines **7**(6), 102 (2016).
[12] Lin, H.-C., Chen, M.-S. and Lin, Y.-H., "A Review of Electrically Tunable Focusing Liquid Crystal Lenses," Trans. Electr. Electron. Mater. **12**(6), 234–240 (2011).
[13] Madec, P.-Y., "Overview of deformable mirror technologies for adaptive optics and astronomy," Adapt. Opt. Syst. III **8447**, B. L. Ellerbroek, E. Marchetti, and J.-P. Véran, Eds., 844705-844705–844718, International Society for Optics and Photonics (2012).
[14] Reddy, G. D. and Saggau, P., "Fast three-dimensional laser scanning scheme using acousto-optic deflectors," J. Biomed. Opt. **10**(6), 064038 (2005).
[15] Benton, D. M., "Multiple beam steering using dynamic zone plates on a micromirror array," Opt. Eng. **57**(07), 1 (2018).
[16] Arnold, C. B., Theriault, C., Amrhein, D., Kang, S. and Dotsenko, E., "Ultra-high-speed variable focus optics for novel applications in advanced imaging," Photonic Instrum. Eng. V **10539**, Y. G. Soskind, Ed., 1, SPIE (2018).
[17] Janin, P., Bauer, R., Griffin, P., Riis, E. and Uttamchandani, D., "Characterization of a Fast Piezoelectric Varifocal MEMS Mirror," 2018 Int. Conf. Opt. MEMS Nanophotonics, 1–5, IEEE (2018).
[18] Song, Y., Panas, R. M. and Hopkins, J. B., "A review of micromirror arrays," Precis. Eng. **51**, 729–761 (2018).
[19] Lapisa, M., Zimmer, F., Niklaus, F., Gehner, A. and Stemme, G., "CMOS-integrable piston-type micro-mirror array for adaptive optics made of mono-crystalline silicon using 3-D integration," Proc. IEEE Int. Conf. Micro Electro Mech. Syst., 1007–1010 (2009).
[20] Watson, G. P., Aksyuk, V., Simon, M. E., Tennant, D. M., Cirelli, R. A., Mansfield, W. M., Pardo, F., Lopez, D. O., Bolle, C. A., Papazian, A. R., Basavanhally, N., Lee, J., Fullowan, R., Klemens, F., Miner, J., Kornblit, A., Sorsch, T., Fetter, L., Peabody, M., et al., "Spatial light modulator for maskless optical projection lithography," J. Vac. Sci. Technol. B Microelectron. Nanom. Struct. Process. Meas. Phenom. **24**(6), 2852–2856 (2006).
[21] Ersumo, N. T., Yalcin, C., Pegard, N., Waller, L., Lopez, D. and Muller, R., "Concentric Micromirror Array for High-Speed Optical Dynamic Focusing," 2019 Int. Conf. Opt. MEMS Nanophotonics (IEEE OMN 2019) (2019).
[22] Scott, A. M., Ridley, K. D., Jones, D. C., McNie, M. E., Smith, G. W., Brunson, K. M., Lewin, A. and Lewis, K. L., "Retro-reflective communications over a kilometre range using a MEMS-based optical tag," Unmanned/Unattended Sensors Sens. Networks VI **7480**, 74800L, International Society for Optics and Photonics (2009).
[23] Wang, Y., Zhou, G., Zhang, X., Kwon, K., Blanche, P.-A., Triesault, N., Yu, K. and Wu, M. C., "2D broadband beamsteering with large-scale MEMS optical phased array," Optica **6**(5), 557–562 (2019).
[24] Martínez, A., del Mar Sánchez-López, M. and Moreno, I., "Phasor analysis of binary diffraction gratings with different fill factors," Eur. J. Phys. **28**(5), 805 (2007).
[25] Shane, J. C., McKnight, D. J., Hill, A., Taberski, K. and Serati, S., "Designing a new spatial light modulator for holographic photostimulation," Opt. Trapp. Opt. Micromanipulation XVI **11083**, K. Dholakia and G. C. Spalding, Eds., 3, SPIE (2019).
[26] Aramendía, A. R., Grulkowski, I., Villar, A. J., Manzanera, S., Chen, Y., Mompean, J., Díaz-Doutón, F., Pujol, J., Güell, J. L. and Artal, P., "Optimization of a SS-OCT with a focus tunable lens for enhanced visualization of ocular opacities," Opt. Coherence Tomogr. Coherence Domain Opt. Methods Biomed. XXIII **10867**, 108673E, International Society for Optics and Photonics (2019).